AGU100 ADVANCING EARTH AND SPACE SCIENCE

Earth's Future

RESEARCH ARTICLE
10.1029/2018EF000825

Key Points:
- Ocean heat content was highest on record just before northern summer of 2017, supercharging Atlantic hurricanes Harvey, Irma, and Maria
- The Gulf of Mexico ocean heat loss during Harvey matched the latent heat released by Harvey rainfall and thereby fueled the storm
- Essential adaptation to the natural hazards and climate change is not happening in many vulnerable areas, with major consequences

Supporting Information:
- Supporting Information S1

Correspondence to:
K. E. Trenberth,
trenbert@ucar.edu

Citation:
Trenberth, K. E., Cheng, L., Jacobs, P., Zhang, Y., & Fasullo, J. (2018). Hurricane Harvey links to ocean heat content and climate change adaptation. *Earth's Future*, *6*. https://doi.org/10.1029/2018EF000825

Received 25 JAN 2018
Accepted 3 MAY 2018
Accepted article online 9 MAY 2018

Hurricane Harvey Links to Ocean Heat Content and Climate Change Adaptation

Kevin E. Trenberth[1], Lijing Cheng[2], Peter Jacobs[3], Yongxin Zhang[1], and John Fasullo[1]

[1]National Center for Atmospheric Research, Boulder, CO, USA, [2]International Center for Climate and Environment Sciences, Institute of Atmospheric Physics, Chinese Academy of Sciences, Beijing, China, [3]Department of Environmental Science & Policy, George Mason University, Fairfax, VA, USA

Abstract While hurricanes occur naturally, human-caused climate change is supercharging them and exacerbating the risk of major damage. Here using ocean and atmosphere observations, we demonstrate links between increased upper ocean heat content due to global warming with the extreme rainfalls from recent hurricanes. Hurricane Harvey provides an excellent case study as it was isolated in space and time. We show that prior to the beginning of northern summer of 2017, ocean heat content was the highest on record both globally and in the Gulf of Mexico, but the latter sharply decreased with hurricane Harvey via ocean evaporative cooling. The lost ocean heat was realized in the atmosphere as moisture, and then as latent heat in record-breaking heavy rainfalls. Accordingly, record high ocean heat values not only increased the fuel available to sustain and intensify Harvey but also increased its flooding rains on land. Harvey could not have produced so much rain without human-induced climate change. Results have implications for the role of hurricanes in climate. Proactive planning for the consequences of human-caused climate change is not happening in many vulnerable areas, making the disasters much worse.

Plain Language Summary Human-induced climate change continues to warm the oceans which provide the memory of past accumulated effects. The resulting environment, including higher ocean heat content and sea surface temperatures, invigorates tropical cyclones to make them more intense, bigger, and longer lasting and greatly increases their flooding rains. The main example here is Hurricane Harvey in August 2017, which can be reasonably isolated in terms of influences on and by the environment. Hurricanes keep tropical oceans cooler as a consequence of their strong winds that increase evaporation. Here we show for the first time that the rainfall likely matches the evaporation and the corresponding ocean heat loss. Planning for such supercharged hurricanes (adaptation) by increasing resilience (e.g., better building codes and flood protection) and preparing for contingencies (such as evacuation routes, power cuts, and so forth) is essential but not adequate in many areas, including Texas, Florida, and Puerto Rico where Harvey, Irma, and Maria took their toll.

1. Introduction

The Atlantic hurricane season in 2017 broke numerous records, with well-above normal activity, especially with the tremendous damage from Harvey, Irma, and Maria. Hurricanes are normal events in summer, with an average of 12 named storms and 6 hurricanes in the Atlantic. However, in 2017 there were 17 named storms and 10 hurricanes, 6 of which were categorized as "major." According to National Oceanic and Atmospheric Administration (NOAA), the accumulated cyclone energy (ACE) was 225% of normal. Several aspects of the 2017 season were not "natural." The first was the role of human-induced climate change, and the second was the role of preparedness. Here we focus on the links between ocean heat content (OHC) and hurricanes in the Atlantic Ocean, highlighting the record heat in the Gulf of Mexico prior to hurricane Harvey in 2017, and then the subsequent evaporative cooling during the storm's passage corresponding to the heavy rainfalls in Harvey. Given that more active Atlantic hurricanes are expected because of climate change, we also provide a brief commentary on the disasters, which occurred despite many warnings.

There is no doubt that the climate is changing primarily because of increased long-lived greenhouse gases, such as carbon dioxide, in the atmosphere that have increased radiative forcing of the climate system (IPCC, 2013; USGCRP, 2017). A consequence is an energy imbalance at the top of the atmosphere (Trenberth et al., 2014; von Schuckmann et al., 2016) of which about 92% goes into the ocean, increasing OHC. Primary

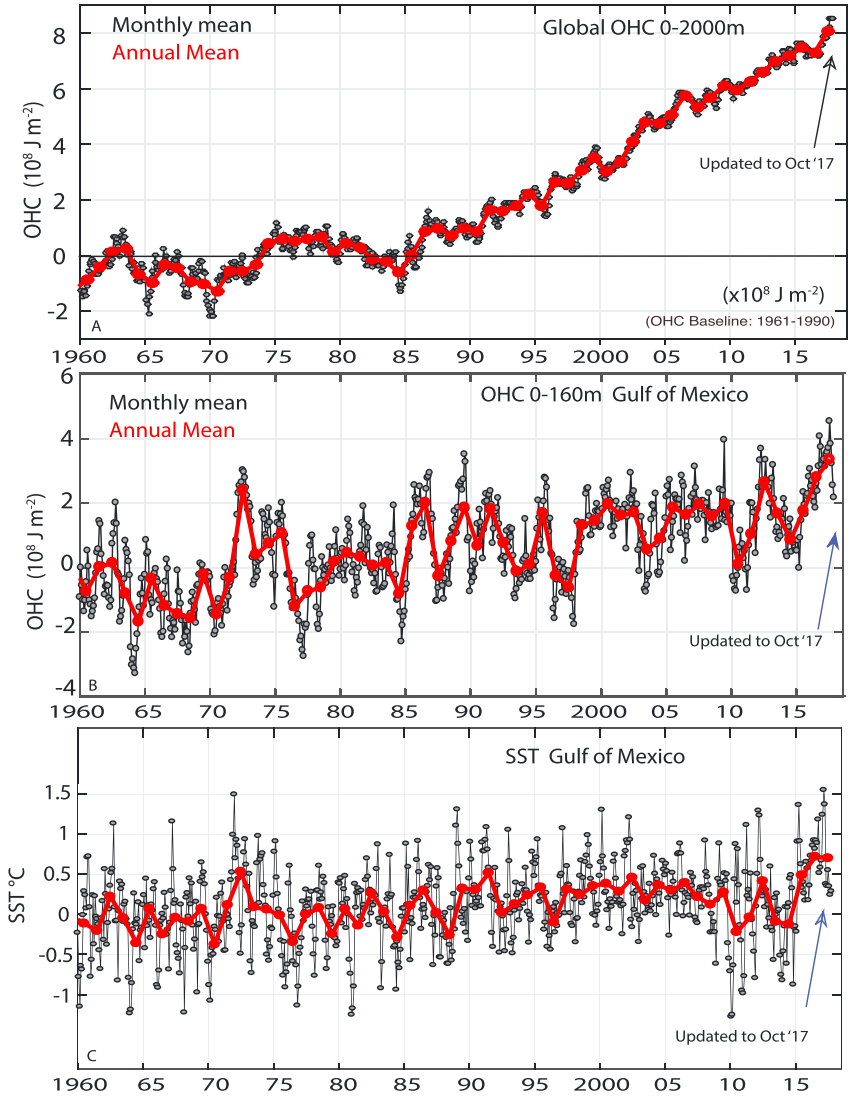

Figure 1. Ocean heat content anomalies for the monthly (black) and annual (red) for (a) the top 2,000 m for the global ocean and (b) for the top 160 m in the Gulf of Mexico (dashed box in Figure 2), in 10^8 J m^{-2}. (c) The sea surface temperature anomalies in the Gulf of Mexico. For all time series, the last month is October 2017 and the last red dot is for January to October 2017. The baseline is 1961–1990.

indicators of a changing climate include increases in global mean surface temperature, sea level, and OHC (Cheng et al., 2017, 2018; Figure 1a). Moreover, OHC and sea level changes are more robust climate indicators with less weather noise, both for global averages (Cheng et al., 2018) and regional changes. The latter is illustrated, for example, in the Gulf of Mexico (Figures 1b and 1c) in this study. Regional changes, especially the loss of Arctic sea ice and glaciers, are also very visible indicators of global warming (USGCRP, 2017). However, changes in certain extremes that have also been linked to such climate change (Trenberth et al., 2003) have a much greater impact on the environment and society (Garner et al., 2017; Lin & Shullman, 2017). These include increased risks of heat waves, drought and wild-fires at one extreme of the hydrological cycle, and increased heavy rains and risks of flooding at the other (Lin & Shullman, 2017; Peduzzi et al., 2012; Trenberth et al., 2003), associated with increased water vapor and higher temperatures in the environment.

Hurricanes form in general over tropical oceans where sea surface temperatures (SSTs) are greater than 26°C. As discussed in section 4.1, the atmospheric conditions need to be favorable, usually with high water vapor

content, weak wind shear (or the vortex comes apart), weak static stability, and with a preexisting disturbance to help organize the convection. In the Atlantic the disturbances typically originate over or near Africa, and the atmospheric conditions all tend to go hand-in-hand with cyclonic conditions. Hence, as discussed in section 4.1, conditions in other parts of the tropics can influence the Atlantic.

It is generally expected that storm and hurricane activity will be affected by climate change, primarily because all storms occur in a warmer and moister environment, increasing precipitation and thus latent heat release, with feedbacks on moisture convergence (Trenberth, 2005; Trenberth & Fasullo, 2007). For tropical cyclones (TCs; including hurricanes or typhoons), the general expectation is for more activity (Emanuel, 2007, 2013; Trenberth & Fasullo, 2008). There may be fewer but more intense storms (i.e., relatively more Category 4/5 storms; Knutson et al., 2015; Knutti & Sedláček, 2012; Sobel et al., 2016), in part because of changes in atmospheric stability, and in part because a few bigger storms can replace many smaller storms in terms of their impact on the ocean (Trenberth & Fasullo, 2008). However, these results largely arise from global modeling experiments which only coarsely resolve tropical storms, whereas dynamically downscaled experiments find increases in both frequency and intensity (Emanuel, 2013).

Tropical storms and hurricanes spin up very strong winds which increase the surface turbulent fluxes, primarily evaporation (latent heat), by an order of magnitude or more (Lin et al., 2008, 2009; Shay et al., 1992; Trenberth et al., 2007). The increased atmospheric moisture flows into the hurricane and fuels the storm itself. As the intensity increases, spiral arm bands become more circular and can form a new eye wall, known as eyewall replacement, where the new eye wall has a much larger radius (Sitkowski et al., 2012). Such eyewall replacements occurred several times in Irma, resulting in a very large hurricane. Hence, while the ocean is the energy source of the storm, the upper ocean cools as heat is mixed downward and especially through evaporative cooling, leaving behind a cold wake (Brand, 1971; Cheng et al., 2015; Emanuel, 2015; Mei & Pasquero, 2013; Price, 1981; Sriver & Huber, 2007) and creating a less favorable environment in the immediate area for subsequent storms (Brand, 1971; Lloyd & Vecchi, 2011).

The process of tapping the upper OHC, and the formation of the cold wake, means that there is a dependence of the sustainability of the storm (lifetime, size, and intensity) on OHC, and higher OHC contributes to more rainfall (Lin et al., 2011). The energy is manifested in both kinetic energy, via high wind speeds, and the intensity of the storm, and latent energy which is realized in the atmosphere as moisture is rained out in heavy precipitation. However, after the storm, the upper ocean cooling can be restored by solar heating within a few weeks (Balaguru et al., 2014; Cheng et al., 2015; Mei & Pasquero, 2013), and other large-scale variability (i.e., global warming, El Niño–Southern Oscillation [ENSO]) may dominate low-frequency changes of OHC, making the examination of links between OHC and TCs difficult. Previous studies using monthly or seasonal data blur the important distinction between the "before" effects of OHC on the storm with the "after" effects of the storm on OHC. Lack of ocean subsurface observations with day-to-day resolution is the main reason for this limitation. Former studies used either indirect ocean subsurface observations (i.e., reconstructed ocean observations from high resolution sea surface height data; Jaimes et al., 2015; Rogers et al., 2017) or a composite method by collecting all Argo data over many TCs to provide a mean ocean response (Cheng et al., 2015).

With Hurricane Harvey fairly isolated over the Gulf of Mexico, there is a unique opportunity to examine the ocean-TC linkages directly from ocean in situ observations. Harvey occurred in an area with record high ocean warming in the Gulf (Figure 1b) and therefore provides the opportunity to study a storm in an environment of anomalous OHC and provides a brief commentary on the role of hurricanes in the climate system. Using the example of Harvey, this study examines the link between OHC and hurricanes from an energy and moisture perspective and also provides a brief commentary on implications for adaptation, given the extreme rainfall and devastation that Harvey caused over land. The data and methods are introduced in section 2. OHC and SST change during Harvey are presented in section 3, followed by a detailed analysis of precipitation. The more general context for the summer of 2017 events is discussed in section 4 along with the importance of the adaptation to natural hazards.

2. Data and Methods

Ocean heat content data are calculated from the Institute of Atmospheric Physics global ocean temperature gridded data set (Cheng et al., 2017) with 1° × 1° spatial and 1-month temporal resolution for the upper

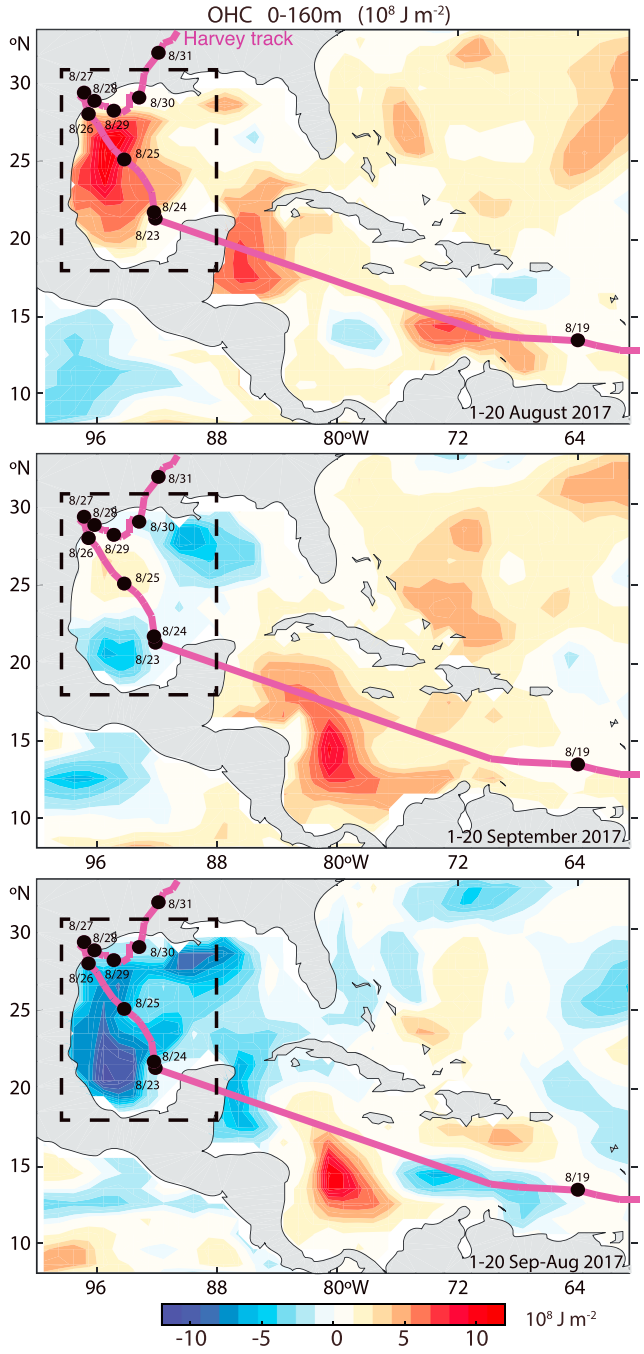

Figure 2. Ocean heat content (OHC) and rainfall in the Gulf of Mexico with Harvey. OHC for upper 160 m as departures from the mean for 1961–1990 for (top) 1–20 August, (middle) 1–20 September, and (bottom) 1–20 September to 1–20 August 2017 in 10^8 J m^{-2}. The tropical cyclone track for Harvey is included. The box indicates the region where the statistics related to the Gulf of Mexico in this study were computed.

0–2,000 m and available from January 1940 to October 2017. This data set includes all of the available ocean temperature observations provided in World Ocean Database, including Argo, expendable bathythermographs, shipboard measurements, moorings, autonomous pinniped bathythermograph observations, etc. In this study, we focus on the OHC for the upper 160 m for different regions including the Gulf of Mexico (18°N–30°N, 88°W–98°W). To calculate OHC change before and after Harvey, we follow the method in Cheng et al. (2017) but perform the reconstruction for two time periods: 1–20 August (before) and 1–20 September 2017 (after), and we remove annual cycle influences by referencing values to the climatology1961–1990. The irregular sampling of the in situ observations may contribute to uncertainty (Figure 3, presented later): The mapping method is designed to average the substantial spatial ocean variability (Cheng et al., 2015; Prasad & Hogan, 2007; Price, 1981) to obtain a reliable net change. Results can also be impacted by the near-inertial (period of 1–2 days) motion of the ocean currents driven by strong storm winds, which induces the up- and down-heaving of the ocean isotherms without involvement of air-sea heat exchange. The mapping method, by averaging all available data over a large area within a time period, reduces the effects of these short-period fluctuations. The uncertainty of OHC change before and after Harvey is derived from the ability of current observations to sample the OHC using a bootstrap method: 80% of the data in the Gulf of Mexico are randomly selected and used to calculate the OHC difference signal, and this is repeated 15 times, and the standard deviation of the results is calculated. We used 2 times the standard deviation ~95% for the significance level.

The use of 0–160 m for the OHC change is consistent with a previous method that assessed the OHC above the 26°C isotherm derived from satellite sea surface height data (Jaimes et al., 2015; Rogers et al., 2017); however we also explore OHC integrated for 300, 700, and 2,000 m depths. Using in situ Argo ocean observations benefits from the high accuracy of direct observations of ocean subsurface conditions.

Monthly SST data from Hadley Center have also been used (Rayner et al., 2003) to examine the SSTs in the Gulf of Mexico (Figure 1c). To investigate SST change before and after Harvey, daily NOAA high resolution SST data are used (see acknowledgments for source and access).

For precipitation, we used estimates from the Global Precipitation Measurement mission product Integrated Multi-satellitE Retrievals for Global Precipitation Measurement (IMERG; Huffman et al., 2014), V4 and V5 (early and final) accessed 29 November 2017 and 8 January 2018. We also used daily/monthly Global Precipitation Climatology Project (GPCP; Huffman et al., 2009) and monthly Global Precipitation Climatology Centre (GPCC; Schneider et al., 2014) analyses of precipitation for comparison, the latter over land only, to help establish uncertainty.

We also use atmospheric data from the global reanalyses from ECMWF Interim Re-Analysis (ERA-I; Dee et al., 2011; see also Trenberth et al., 2011) and the North American Regional Reanalysis (NARR; Mesinger et al., 2006). The latter has 32-km resolution every 3 hr for North America and has the potential advantage of assimilating precipitation data from land stations. For the top-of-atmosphere (TOA) radiation, we used the CERES data set (Loeb et al., 2009) as the climatology plus the operational FLASHFlux product to cover the period of the hurricane.

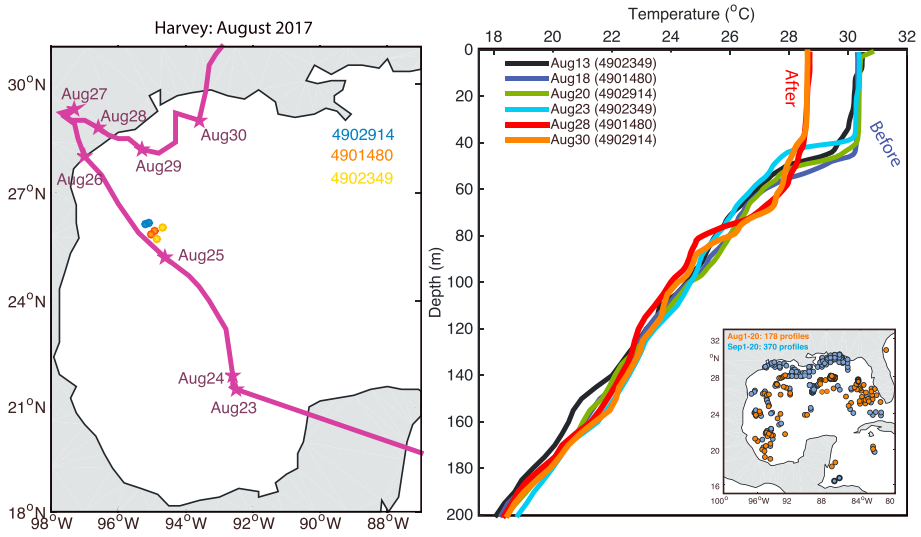

Figure 3. Argo observations under Harvey. (left) Locations of three Argo floats related to Harvey; the numbers are the Argo series numbers, used to identify the Argo float. (right) Temperature profiles observed by the three Argo floats before (observation dates: 13, 18, 20, and 23 August) and after Harvey (observation dates: 28 and 30 August). The inset gives the overall distribution of the profiles for 1–20 August (178, orange) and 1–20 September 2017 (370, blue).

3. Results

3.1. OHC, SST, and Hurricane Harvey

Harvey developed to the east of the Windward Islands, reaching tropical storm status on 17 August until 1 September 2017 (Figure 2); see Blake and Zelinsky (2018). It passed over the Caribbean Sea from 17 to 23 August and began to rapidly intensify on 24 August, becoming a hurricane the same day. Moving generally northwest, Harvey further intensified on 25 August to become a major hurricane of Category 4 intensity. Hours later, Harvey made landfall near Rockport, Texas, at peak intensity. The increase in strength and size meant that even after landfall, its circulation extended well out over the Gulf, where a continual flow of moisture fed and prolonged the storm, long after most storms would have died. (P. Klotzbach [personal communication 2018] found in a study that the median time of Texas landfalling hurricanes before weakening below tropical storm strength is 27 hr.) Certainly, the track of Harvey was unusual, but it was likely governed mostly by the synoptic weather situation.

Heat from the ocean provides the fuel for hurricanes. Accordingly, ocean heat loss after Harvey would be expected. In the weeks prior to Harvey in 2017, OHC was at a record level in the Gulf of Mexico (Figures 1b, 2, and 3), and very high SSTs (>30°C) set the stage for Harvey (Figure 4). A comparison of OHC after Harvey for 1–20 September with 1–20 August before Harvey in the Gulf (Figure 2) reveals that OHC to 160 m depth (OHC160) was abruptly reduced by Harvey by $5.93 \pm 0.97 \times 10^{20}$ J where the uncertainty is 2 times the standard deviation. This is a monthly ocean heat loss of ~0.23 PW in the Gulf, equivalent to 201 W m^{-2} over 31 days.

These changes in OHC may have also been influenced by other TCs in August (Franklin) and September (Irma, Katia) while still others affected the areas farther east (Gert, Jose, Lee, and Maria) in the Atlantic Ocean and Caribbean in September. These effects add to the uncertainty of our calculation, but most of the strong hurricanes were outside the Gulf region. Only Katia was in the Gulf but within 20–22.5°N. With its relatively small size and short duration it might have contributed a small amount of OHC decrease in the Gulf. To approximately assess an upper limit to Katia's impact, we calculate the OHC change south of 22°N in the dashed box in Figure 2, and the OHC decrease from 1–20 August to 1–20 September is $1.32 \pm 0.97 \times 10^{20}$ J, but this also includes effects from Harvey which was near 21°N from 23 to 24 August.

Large-scale variability, such as ENSO, could also contribute to the observed OHC changes in the Gulf of Mexico. For example, OHC in the Gulf of Mexico tends to decrease several months following the peak of

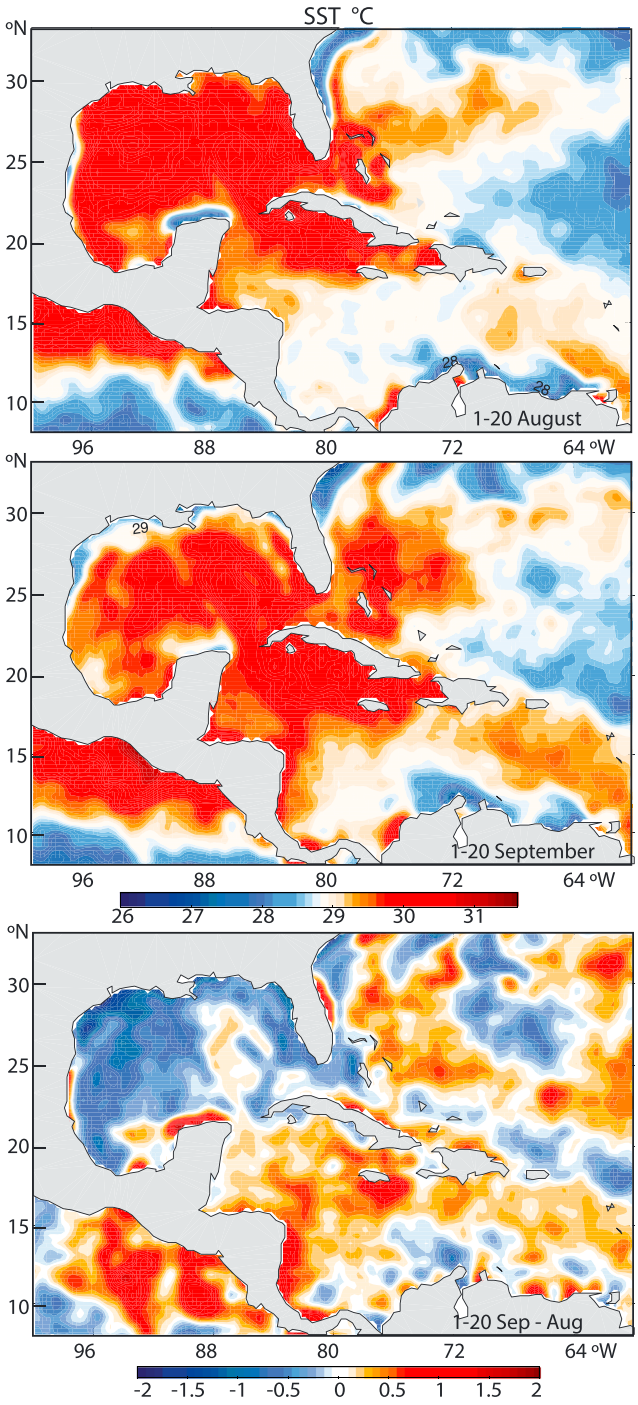

Figure 4. Sea surface temperatures for (top) 1–20 August and (middle) 1–20 September 2017. (bottom) Anomaly difference between 1–20 September and 1–20 August after removing the daily climatology in °C.

El Niño. Regression between temperature change in the Nino3.4 region (using the Oceanic Niño Index) and the OHC160 tendency in the Gulf of Mexico shows a weak but insignificant decrease of OHC160 after El Niño with 5–6 months lag. Moreover, regions outside of the Gulf box (Figure 2) experienced a very weak OHC increase of ~0.93 × 10^{20} J for the upper 160 m during the same period. Hence, it is evident that Harvey was responsible for most of the Gulf cooling.

Indeed, in general TCs extract heat from the ocean, mainly via evaporative cooling and also mix heat in the vertical (Emanuel, 2003; Trenberth et al., 2007). Vertical mixing merely redistributes heat, however, and can be assessed by integrating to greater depths. For the box over the Gulf of Mexico, the OHC change for 300 and 700 m depths was 7.07 ± 1.13 × 10^{20} and 8.77 ± 1.11 × 10^{20} J, respectively, both somewhat larger than the cooling for the top 160 m. This indicates that mixing was not a factor in cooling the top 160 m, and instead, other large-scale processes, such as Ekman pumping, played a role. It is likely that the strong cyclonic winds in Harvey created near-surface divergence of ocean waters, and this upwelling may be responsible for the increased cooling as the depth is increased. As a counter to that, there is likely to be some downwelling in the region farther east from Harvey where clear sunny skies further boost heating, giving rise to the modest increase in OHC.

The continuous heat pump from the ocean by Harvey makes it a self-contained storm. As observed by several Argo floats (Figure 3), near-surface temperatures were >30°C before the storm passage; see also Figure 4. After the storm passage, the near-surface ocean temperature (Figure 3) was reduced by 2°C but was still ~28.5°C and thus larger than the SST threshold for TCs. SST observations by satellites (Figure 4) also show a broad region in the Gulf of Mexico with SST >30°C before Harvey (1–20 August) and an average cooling of ~1 to 2°C after Harvey (compare 1–20 September with 1–20 August; Figures 3 and 4). This suggests that the "cold wake" was not cold enough to significantly suppress the TC intensity, enabling Harvey to continue while over land as the warm ocean conditions still facilitated storm development. The implication is that the warmer oceans increased risk of greater hurricane intensity and duration.

3.2. Rainfall

Harvey's record-shattering rainfall (Risser & Wehner, 2017) featured several locations with over 60 inches (1,500 mm). Emanuel (2017) has shown how the probability of exceptionally high rainfalls in Harvey-like storms has increased because of climate change, and Risser and Wehner (2017) found, using an extreme value analysis, that climate change had increased Harvey precipitation over land by about 37.7%, as a best estimate. van Oldenborgh et al. (2017) found that global warming made the precipitation in Harvey 15% (8 to 19%) higher using a coarse resolution model. Both of these studies were based on past data and found that Harvey was an extremely rare event, but they did not deal with the dynamics or environment of the specific event. Wang et al. (2018) did account for the dynamics of the situation using model experiments and found a 20 or 26% (13 to 40%) (depending on the days) increase in precipitation. Magnusson et al. (2017) evaluated the performance of the ECMWF high resolution forecast model in predicting the intensity and rainfall in Harvey and showed that while the intensity was not well reproduced in forecasts, the heavy rainfalls over Texas were robust and well replicated, highlighting the fact that they did not depend on details of the storm, but rather depended more on the ocean conditions (i.e., SST) and water

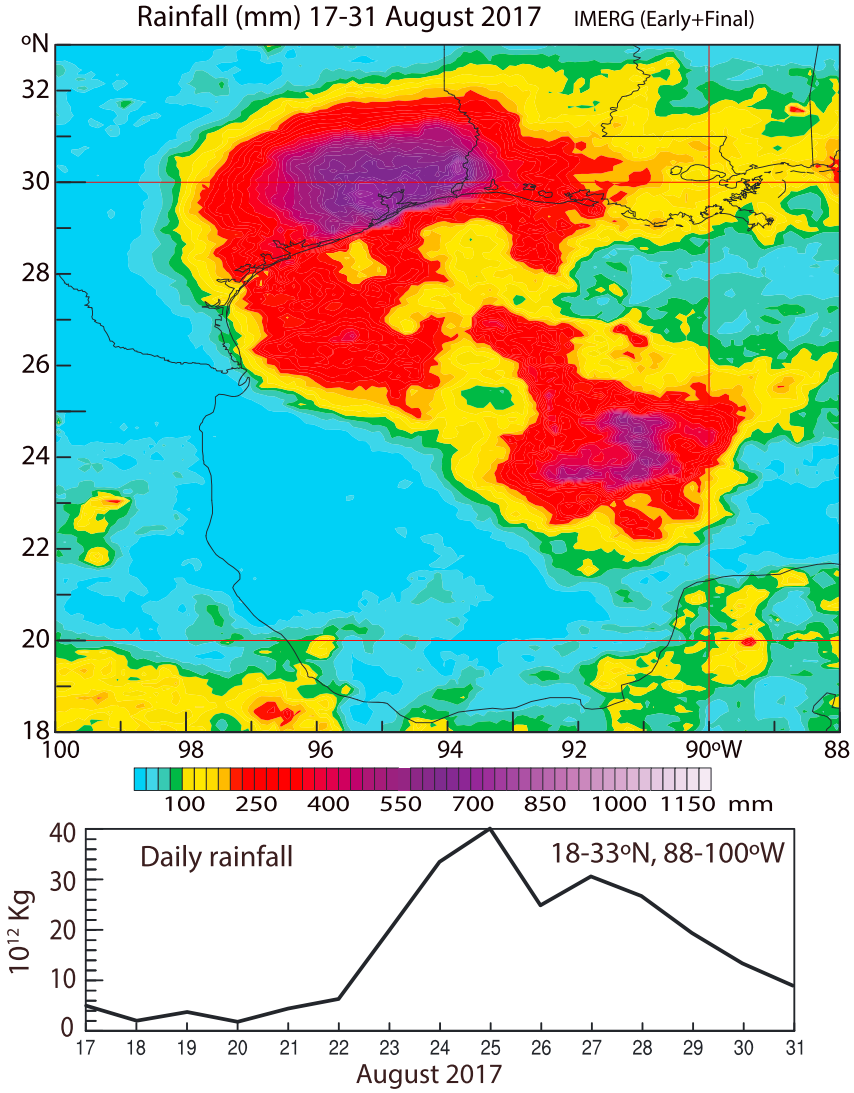

Figure 5. Harvey rainfall accumulated from (top) 17 to 31 August 2017. The values are from Integrated Multi-satellitE Retrievals for Global Precipitation Measurement "early" from 17 to 26 August and "final" 26 to 31 August. (bottom) Daily time series of total precipitation integrated over the region indicated for 17–31 August 2017 in 10^{12} kg. Ten units is 7.55 mm.

vapor in the atmosphere. The performance was better in the high-resolution model than the lower-resolution ensemble mean forecast.

For the 17–31 August, an estimate of the total precipitation (Figure 5) has about half of the area subject to substantial rainfall and most rainfall occurred after 23 August. However, there is considerable uncertainty in the rainfall estimates. For IMERG, there are several products produced to satisfy operational needs, and a "final" product is produced a few months later. There are considerable differences between the early IMERG and the "final" data. The early data showed significantly higher precipitation over the ocean prior to 26 August, while the "final" values are higher over land. Accordingly, we have combined them to assess the uncertainties and which fields are more likely. The "final" product appears inconsistent with the OHC losses. Figure S1 in the supporting information presents four different estimates using IMERG and GPCP, with the latter much coarser in resolution, and the total area averages are given in Table 1.

From 18 to 33°N 88–100°W from 17 to 31 August the average rainfall was 120 mm, or 2.4×10^{14} kg over an area of 2.0×10^{12} m^2. This gives rise to 6.0×10^{20} J of latent energy in rainfall which has to come from the in

Table 1
Total Precipitation 18–33°N, 100–88°W From Various Products for the Dates Given and Combined in kg, then Converted to mm by Dividing by the Area (Which Differs Slightly for GPCP) and in Latent Heat Units

Units	10^{11} kg		mm	10^{20} J
Dates	17–25 August	26–31 August	17–31 August	
IMERG early	1,162.7	1,085.1	2,247.8	112.2	5.63
IMERG final	837.4	1,235.4	2,072.8	103.5	5.19
Early + final	1,162.7	1,235.4	2,398.1	119.7	6.00
Final + early	837.4	1,085.1	1,922.5	96.0	4.81
GPCP	1,003.0	1,250.1	2,253.1	93.4	5.64

Note. GPCP, Global Precipitation Climatology Project; IMERG, Integrated Multi-satellitE Retrievals for Global Precipitation Measurement.

situ ocean plus the moisture convergence from the adjacent areas in both the ocean and atmosphere (Trenberth & Fasullo, 2007, 2008).

To further assess the uncertainty in the precipitation, we compared several products over land only for the period of 1–31 August 2017 (GPCC, GPCP and IMERG [final]). For the land 27 to 33°N, 100–89°W, an area of 5.97×10^{11} m^2, the values range from 1,477 to 1,518 to 1,588 $\times$ 10^{11} kg (247 to 266 mm), with IMERG in the middle. Hence, the two standard deviations of the three values is 112×10^{11} kg (consistent with the range of the three values: 7.3%), and the spread about the IMERG value is +4.6% to −2.7%. For the whole area for the period of 17–21 August (Table 1), GPCP gives 5.64×10^{20} J, which is more consistent with the early IMERG, while our combined product (Figure 5) has 6.0×10^{20} J, which is an excellent match to the energy loss in the top 160 m of the ocean beneath the storm.

3.3. Energy and Moisture Budgets

The climatological mean August 2001 to 2016 net surface energy flux for the Gulf of Mexico ocean box (18–30°N 88–98°W) is −33 W m^{-2} (i.e., into the ocean, with 1 standard deviation uncertainties of ±10 W m^{-2}) based on our heat and water budget studies (e.g., Trenberth & Fasullo, 2017). The annual mean net surface flux is higher, about −50 W m^{-2}, and this signifies a divergence of ocean heat transport within the ocean, some of which feeds the northward heat transport in the Gulf Stream.

Similarly, based upon our budget analysis, the climatological mean net surface radiative fluxes are 195 W m^{-2} downward, primarily because of the strong sunshine, and the net turbulent fluxes are 162 W m^{-2} upward. Yu and Weller (2007) and Pinker et al. (2014) present a breakdown of surface fluxes using conventional means and show that because the sensible heat flux is very small (typically less than 10 W m^{-2} in August), the net turbulent surface flux is dominated by the latent heat flux. For Katrina (Trenberth & Fasullo, 2007), the sensible heat flux was a factor of 5 to 10 less than the latent heat flux.

In our study, we computed the OHC loss over a month, from 1–20 August to 1–20 September 2017, as 8.8×10^{20} J for the top 700 m, and subtracting the increase in the surrounding area gives 7.8×10^{20} J. If we assume that the net surface flux is about zero for the 16 days outside of 17–31 August, then the anomalous cooling from the implied net surface flux over the Gulf of Mexico ocean box for 17–31 August is 550 W m^{-2}. The net radiation anomalies, as discussed below, are small (−3 W m^{-2}). Because the SSTs were slightly higher than the surface air temperatures (Blake & Zelinsky, 2018), the sensible heat flux contributes, and from NARR is 8 W m^{-2}. Further allowing for an ocean heat divergence of 33 W m^{-2} reduces the estimated evaporative latent heat flux to about 500 ± 77 W m^{-2}. This moistens the atmosphere.

The rainfall amount for the area 18–33°N 88–100°W for 17–31 August (Figure 5) is equivalent to 421 ± 30 W m^{-2} if applied to the ocean area in the Gulf box. Some moisture is transported outside of that box, especially to the east in the quasi-stationary front near the Gulf coast (Figure S2), and some is retained in the atmosphere for subsequent rainfall farther north as the remnants of Harvey progressed northward in September.

We have attempted to provide insights into the moisture budgets using ERA-I and NARR reanalyses. Unfortunately, neither is very helpful in providing closure for Harvey as their depiction of the storm was

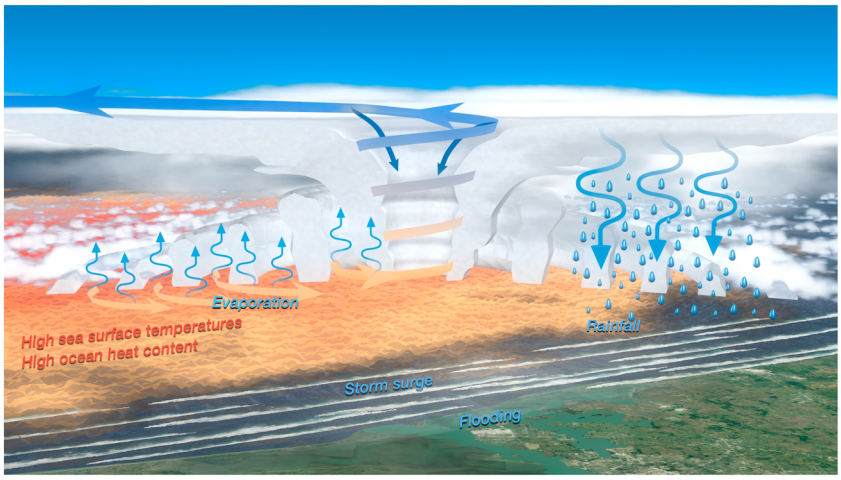

Figure 6. Schematic cross section of a hurricane occurring over very high sea surface temperatures and high ocean heat content that increase evaporation (blue thin arrows). The moisture converges (orange arrows) into the storm leading to heavy precipitation (blue drops at right) and adding buoyancy to the air. The moisture as rain, along with any storm surge, causes surface flooding. The outflow from the storm at upper levels is also depicted. (Courtesy Steven Deyo, NCAR).

poor. ERA-I analyzed the minimum surface pressure to be 1,000 hPa versus observed 937 hPa (Blake & Zelinsky, 2018). For NARR the analyzed minimum sea level pressure was 988.3 hPa. Even the higher resolution operational models at ECMWF performed poorly in terms of intensity forecasts (Magnusson et al., 2017). Nonetheless, we have computed the vertical integrals of the atmospheric moisture transports and their divergence (Figure S2). The latter are equal to the surface evaporation E minus the precipitation P, plus a small atmospheric storage (tendency term), which we also compute (e.g., Trenberth et al., 2011). Usually the E-P from the moisture budget is more realistic than either the E or P fields (Trenberth & Fasullo, 2013), but not in this case. Instead, the E-P budget results (Figure S2) are quite anemic in both cases. Moisture convergence must play a substantial role over land near Houston, but values are only up to 500 mm, implying large evaporation (over 400 mm), given the precipitation, whereas the E from the reanalyses is less than 80 mm (not shown). Over the ocean south of Texas the reanalysis E was up to about 160/120 W m^{-2} (ERA-I/NARR) which is much too small, because the moisture convergence plus the surface evaporation do not come close to accounting for the observed precipitation. The moisture budgets in the reanalyses are not closed. It suggests that both the surface fluxes and moisture convergence were greatly underestimated by the reanalyses, consistent with the much too weak hurricane winds.

The TOA radiation for the Net, reflected shortwave (RSW), and outgoing longwave (OLR), where the Net = $-$RSW $-$ OLR is downward, is given in Figure S3. There is strong cancellation between the RSW and OLR, as is common in the tropics with convection because high top clouds block (reflect) the Sun, but because the cloud tops are cold, they have low OLR (Trenberth et al., 2015). The absence of convection, as in the southwest of the domain presented, exhibits the reverse sign of anomalies. There is a strong signature of Harvey imprinted on these fields, and clearly, the RSW is much stronger than the OLR, hence contributing to a cooling of the atmosphere-ocean below. In other words, the extensive bright cloud from Harvey reflected the strong summer sunshine back to space, and this solar radiation would normally heat the ocean. However, the area average is only -3 W m^{-2}, which is 8×10^{18} J for the 15-day period, more than an order of magnitude less than the OHC loss and latent heat release.

We also computed the total column atmospheric energy divergence every 6 hr for August 2017 (Trenberth & Fasullo, 2017; not shown), which is quite noisy for such a short period and has large uncertainty as it is not mass-budget corrected, but averaged over the region for 17–31 August is about 160 W m^{-2}. Applying this over a region 3 times that of the ocean box is sufficient to account for the latent heat energy dispersion. Hence, through the atmospheric circulation, the latent heat and TOA radiation effects of Harvey are dispersed over a much wider area (illustrated in Figure 6) and difficult to isolate. Overall for this domain, the radiation contributes little to the overall OHC tendency, but it does help offset some latent heat release.

The bottom line is that the total observed OHC change is remarkably compatible with the total energy released by precipitation and, unsurprisingly, reflect strong energy exchanges during the hurricane. Accordingly, the record high OHC values not only increased the latent heat which fueled the storm itself, likely increasing its size and intensity, but also likely contributed substantially to the flooding caused by rainfall on land. The implication is that if the OHC had been less, then the rainfall amounts would also have been less (as has been found for typhoon Morakot, Lin et al., 2011).

Given that SSTs have increased about 0.6°C since 1960 due to anthropogenic climate change (as seen in Figure 1), there is on average about 5% more moisture in the atmosphere (Trenberth et al., 2005). This converts directly into increased rainfall through the moisture convergence, but it also invigorates and enlarges the storm, so that the net increase is expected to be a factor of 2 to 4 larger in the absence of other effects (Trenberth et al., 2003). For Harvey the amplification has been found to be about 37.7% (Risser & Wehner, 2017) or 20 or 26% (depending on days) (13 to 40%; Wang et al., 2018). A 35% increase in rainfall from climate change would thus be as much as 15 inches (380 mm) in places.

4. Discussion

4.1. Link Between Hurricanes and a Warming Ocean

Because a warmer ocean supports more TC activity, we briefly explore relationships with OHC more generally. Increases in Atlantic hurricane activity in the 20th century have been attributed mainly to the increases in tropical Atlantic SST over the main TC development region of 6°–18°N, 20°–60°W in the hurricane season, which is primarily driven by human increases in greenhouse gas concentrations (Emanuel, 2005; Mann & Emanuel, 2006; Trenberth & Fasullo, 2008; Villarini & Vecchi, 2012). Over the north tropical Atlantic Ocean (0–30°N), OHC increased substantially in the TC season in the past five decades at a rate of 0.07×10^8 J m^{-2} per year for 1970–2017. These increases are linked to the global OHC increases (Figure 1) and undoubtedly are caused by human-induced climate change, as discussed in the introduction.

Both SST and OHC are projected to increase in the future (IPCC, 2013); there will be a warmer and wetter world over oceans and more energy available for evaporation (Emanuel, 2017; Trenberth & Fasullo, 2007; USGCRP, 2017; Yamada et al., 2017), facilitating more TC activity and more rainfall (Emanuel, 2017; Knutson et al., 2010, 2015; Knutti & Sedláček, 2012; Vecchi & Soden, 2007; Walsh et al., 2015; Yamada et al., 2017). The question is whether the atmospheric conditions, in particular its stability and wind shear, also remain favorable, but these are likely at least episodically because convection plays a major role in stabilizing the atmosphere. The evaporative cooling of the ocean by strong winds in the TC moistens the atmosphere giving rise to latent energy that is realized when rainfall occurs, thereby fueling the storm when the water vapor condenses to form clouds and rain, warming the surrounding air. Flooding is then expected if the rainfall is over land, and both heavy rains and flooding can extend considerable distances inland. Therefore, a warming ocean will facilitate more TC activity and more rainfall and flooding, which is well supported by the Harvey case.

However, both hurricane activity and regional OHC experience substantial variability (Vecchi & Soden, 2007) on interseason, interannual to decadal time scales (Figure 1b). Physically, the dependence of hurricanes on high SSTs is well-established as a necessary, but not sufficient, condition. Because thresholds are involved, a linear relationship between OHC and hurricane activity is not expected; if the OHC and SSTs are low, there is little activity below a certain level. SST differences also play a major role by favoring one geographical region over another and thus determining preferred cyclonic regions for where storms develop. Another requirement is an atmospheric disturbance (Bell & Chelliah, 2006). Climate and statistical models have successfully simulated changes in numbers of TCs in the Atlantic, given just SSTs (Chen & Lin, 2011; LaRow et al., 2010; Vecchi et al., 2011), indicating that atmospheric factors such as wind stress and atmospheric stability can largely be accounted for by the tropical atmospheric circulation changes driven by SST patterns and the underlying OHC. The biggest single interannual factor globally is ENSO, whereby the TC activity is favored in the Pacific during El Niño while in the Atlantic activity is somewhat suppressed. The Atlantic activity increases during La Niña conditions, especially when unleashed after a period of suppression (such as occurred in 2015 to May 2016). The actual TC activity in a given basin depends both on other basins and competition for where activity should be. Nevertheless, the potential for more activity as OHC relentlessly rises is clear.

It is evident in our results that hurricane Harvey cooled the ocean substantially. Even though solar radiation can replenish lost heat quickly in upper layers, a role of hurricanes in the climate system is to keep tropical oceans cooler than they otherwise would be (Trenberth & Fasullo, 2007). Hurricanes provide an effective thermal relief valve for the tropics. This also suggests that climate models that do not contain hurricanes (i.e., all of them) cannot expect to get the SSTs and OHC correct either today or in the future, and this raises serious questions whether future SSTs may be somewhat lower but at the expense of more TC activity.

Hurricane Harvey has provided a unique case to enable the before and after effects of the OHC and SSTs on and by the storm to be isolated. Consistency between ocean heat loss and precipitation during Harvey provides strong evidence for the role of ocean in the hurricane evolution, intensity, and prodigious rains (and flooding) and has important implications for the future.

4.2. Adaptation to Climate Change

With climate change, the foci of efforts such as through the Paris Agreement in December 2015 have been first on "mitigation," meaning reductions in greenhouse gas emissions to slow or stop the problem, and second on "adaptation," to build resilience and plan for the inevitable impacts. The third option being realized in many places is to suffer the consequences!

The threats from increasing hurricane activity with climate change have been reasonably well established since intensive research following Katrina in 2005 (Emanuel, 2005; Trenberth et al., 2007; Trenberth & Fasullo, 2008) and assessed in IPCC (2013). Meetings have been held in the Caribbean of local politicians and the public expressing concern about the risks from higher sea levels and stronger hurricanes (e.g., Ramkissoon & Kahwa, 2015). Why then was there not better preparedness that builds resiliency to expected conditions? Houston has been beset with three 500-year floods in 3 years prior to Harvey, and Miami regularly experiences "sunny day" flooding with high tides. Why was there reportedly only 1 in 6 with flood insurance in the Houston area and Florida? Why have various flood mitigation measures not been enacted? The hurricanes of the summer of 2017 in the Atlantic are yet another example of how disaster risk management and climate adaptation, while challenging for multiple reasons, remain critically important.

Houston has experienced unbridled growth, much of it in floodplains, without zoning restrictions or planning for adequate drainage or building codes. The *New York Times* (Kimmelman, 2017) featured the Houston development: "Built on a mosquito-infested Texas swamp, Houston similarly willed itself into a great city. For years, the local authorities turned a blind eye to runaway development. Thousands of homes have been built next to, and even inside, the boundaries of the two big reservoirs devised by the Army Corps of Engineers in the 1940s after devastating floods. Back then, Houston was 20 miles downstream, its population 400,000. Today, these reservoirs are smack in the middle of an urban agglomeration of six million."

In the wake of Hurricane Ike, which claimed 113 lives in Galveston Bay in 2008, proposals for large-scale flood control projects in the Houston area were rebuffed, and Houston residents have voted 3 times not to enact a zoning code. The mantra has been low taxes and minimal government. Yet there have been many studies that demonstrate how extreme weather, such as the hurricanes, can have a huge human, social, and environmental cost, and it often affects the low-income populations the most (Morss et al., 2011) because they are the most vulnerable (Kelly & Adger, 2000). Adaptation typically requires assessing vulnerability and potential impacts of an event, such as a hurricane, and taking measures to reduce the vulnerability. However, in a given area like Houston, the risk varies considerably and there are many who came through the storm largely unscathed, while others lost nearly everything. The rapid unbridled growth of Houston and building in floodplains means that some residents were much more vulnerable than others.

Irma broke many records including the longest lifetime as a Cat. 5 storm, and it generated the most ACE of any storm in the tropical Atlantic. It was unprecedented in the way it straddled Florida affecting the whole peninsula as it moved northward. Damages from Harvey and Irma are expected to run into hundreds of billions of dollars (for instance by Munich Re; Ellenrieder, 2017; NOAA, 2017). Nevertheless, even greater property and environmental damage occurred both from Irma and then Maria in Caribbean Islands and Puerto Rico. Unlike on the mainland, there was limited mobilization, and restoration of basic services has taken months. Other countries, including Cuba, have somewhat decentralized electricity to build more resilience after 2007. Obsolete "public" utilities and their rules that forbid the use of microgrids and restrict use of solar and wind power are a primary cause (Branson & Lovins, 2017).

The challenge of building resilience and preparing for an event that may or may not come is fraught with perceived risk and burdened by human nature, and there are not simple solutions. Morss et al. (2011) discuss this more generally and highlight the fact that some vested interests even work against better risk management. There is often the issue of a short-term gain versus longer-term security for something that may not happen that comes into play. Also, why should one area, where the perceived risk is less, pay for mitigation in a floodplain where the risk is high?

Hence, not only were these disasters not natural, they were predictable in a general sense, but the preparation for their eventuality has been quite inadequate in hindsight. There is a great need for better planning and building adaptive capacity (Morss et al., 2011) that increases engineering mitigation measures (such as levees and seawalls and flood control), adheres to building codes, prevents building in floodplains, stops unbridled growth, hardens infrastructure, manages water and drainage systems, develops emergency response plans including evacuation routes and their implementation along with emergency shelters and power supplies, and provides property and flood insurance that matches the true and changing risk. Of course, many of these mitigation paths require resources, and some may prove to be inadequate, such as the failure of levees with Katrina in 2005 (Kunreuther, 2006), but in general the benefit to cost ratio is thought to be high, although often the benefits cannot be ascribed a monetary value, and often, they cannot be defined at all (Kunreuther et al., 2013). Given the price tag with units of hundreds of billions of dollars for the recent hurricanes, a modest (two orders of magnitude less) investment in building resiliency may well have saved billions and a lot of grief.

5. Concluding Remarks

Although the effects of climate change arise primarily because of the changing atmospheric composition, the instantaneous effects are small and the main effects arise through the changed environment, especially the warmer oceans. The relentless increases in global OHC (Figure 1) that have made 2017 the warmest year on record for the global ocean have consequences for the atmosphere and climate. Not only are the SSTs higher, but they are supported by the warmer ocean below the surface, enabling sustained effects to occur. This is especially relevant for hurricanes which feed off of the warm tropical waters and drive strong air-sea interactions that involve the ocean subsurface. Indeed, it can be argued that a role of hurricanes in the climate system is to increase the evaporative cooling of the ocean, thereby acting as a cooling valve for the tropical oceans by means of the strong winds and an order of magnitude increase in evaporation. That moistens the atmosphere, and the convergence of moisture into a storm not only leads to higher precipitation but also, for certain storms, greater intensity and growth. Although the latter is less clear for extratropical storms, because the main precipitation is not in the center of the storm, it is especially relevant for hurricanes such as Harvey, Irma, and Maria.

Hurricane Harvey was reasonably isolated in both space and time allowing "before" and "after" assessments of the environment. The very high SSTs were sustained, in spite of Harvey, by the high OHC in the Gulf of Mexico. In regions of this size, there is considerable natural variability associated with TCs and natural variability, but nonetheless, the rising trend that is so much more obvious globally (Figure 1) is evident and caused by human-induced climate change. The increased surface winds in a TC greatly increase evaporation (Figure 6) which provides moisture that spirals into the center of the storm, fueling the updrafts in the eyewall and spiral arm-bands through the latent heat release in heavy precipitation. The TC as a collective of thunderstorms spins up under such favorable conditions and may intensify and expand in size. The larger size of Harvey meant that it could still reach out to the Gulf even after making landfall, and one spiral arm-band brought prodigious amounts of rainfall over Houston. The schematic figure (Figure 6) attempts to capture some of the key ingredients in such storms.

Here we have shown that Harvey took considerable amounts of heat out of the ocean and it was manifested mainly as heavy rainfall. The connections between the rainfall latent heat and OHC loss represent a new approach for understanding the coupled nature of hurricanes. It also suggests that the estimates of water cycle and evaporation from various sources may be quite deficient. This study demonstrates that the coupling of the atmosphere to the ocean is an essential part of the hurricane, which should not be treated solely as a meteorological phenomenon. It also suggests a likely role for hurricanes in the climate system. We have also shown the tremendous benefits of the ocean observing system as given especially by Argo floats. It

allowed the analysis of the ocean changes in new ways. The physics of the phenomenon also suggests that certain rainfall estimates are deficient and that there is scope for considerable improvement, but also that by combining many data and variables, a much more complete picture emerges.

Hurricanes form naturally, and come in all sizes, locations, and tracks, and the activity can be manifested in several ways, through the intensity, size, lifetime, and number of the storms, and good statistics exist for only a few of these variables. Climate change is expected to increase the activity as a whole, but there is competition among basins for where this occurs, and, because it can be manifested in several ways whose integral effects are poorly measured (e.g., ACE does not address storm size), there remains considerable uncertainty over just what has happened and can be expected in the future. Nevertheless, the risk is clear, and preparations for expected effects of climate change on hurricanes and more generally are woefully inadequate. We cannot keep putting off the need to build more resilient systems (Stone, 2018) just because it is required sometime in the future. While destruction from hurricanes is expected, the fact that hurricanes are bigger and stronger means that absolute thresholds are crossed, and catastrophic damage can occur in a nonlinear fashion, as has been witnessed for the three hurricanes in the Atlantic in the summer of 2017. Consequently, while the climate change effect on rainfall may be generally assessed as 5 to 15%, it is not just an incremental cost, but rather the bulk of the whole cost may most appropriately be ascribed to climate change, in this case hundreds of billions of dollars.

Acknowledgments

L. Cheng is supported by the National Key R&D Program of China (2017YFA0603202). This research is partially sponsored by DOE grant DE-SC0012711. NCAR is sponsored by the National Science Foundation. Many thanks to John Abraham and Rebecca Morss for comments and suggestions. OHC data are available at http://159.226.119.60/cheng/. Argo data are available at http://doi.org/10.17882/42182 and we thank the Argo Project http://www.argo.ucsd.edu/Acknowledging_Argo.html. NOAA High Resolution SST data were provided from https://www.esrl.noaa.gov/psd/ by the NOAA/OAR/ESRL PSD, Boulder, Colorado, USA. We use monthly TOA Clouds and the Earth's Radiant Energy System (CERES) Energy Balanced and Filled (EBAF) Ed. 4.0 radiation on (Loeb et al., 2009) http://ceres.larc.nasa.gov/order_data.php and the operational FLASHFlux product from Langley Atmospheric Science Data Center https://ceres.larc.nasa.gov/products.php?product=FLASHFlux. The atmospheric data are the global reanalyses from ECMWF Interim Re-Analysis (ERA-I; Dee et al., 2011) http://data-portal.ecmwf.int/data/d/interim_daily/ and the North American Regional Reanalysis (NARR; Mesinger et al., 2006) https://www.esrl.noaa.gov/psd/data/gridded/data.narr.html. The GPCP version used is 1DD (1 degree daily) V1.3. available at https://www.ncei.noaa.gov/data/global-precipitation-climatology-project-gpcp-daily/access/.

References

Balaguru, K., Taraphdar, S., Leung, L. R., Foltz, G. R., & Knaff, J. A. (2014). Cyclone-cyclone interactions through the ocean pathway. *Geophysical Research Letters*, *41*, 6855–6862. https://doi.org/10.1002/2014GL061489

Bell, G. D., & Chelliah, M. (2006). Leading tropical modes associated with interannual and multidecadal fluctuations in North Atlantic hurricane activity. *Journal of Climate*, *19*, 590–612. https://doi.org/10.1175/jcli3659.1

Blake, E. S., & Zelinsky, D. A. (2018). Hurricane Harvey. National Hurricane Center Tropical Cyclone Rep. AL092017. https://www.nhc.noaa.gov/data/tcr/AL092017_Harvey.pdf. 76 pp.

Brand, S. (1971). The effects on a tropical cyclone of cooler surface waters due to upwelling and mixing produced by a prior tropical cyclone. *Journal of Applied Meteorology*, *10*, 865–874.

Branson R., & Lovins A. B. (2017). How to keep the lights on after a hurricane. New York Times. Oct. 23, 2017. https://www.nytimes.com/2017/10/23/opinion/hurricane-puerto-rico-electricity.html

Chen, J.-H., & Lin, S.-J. (2011). The remarkable predictability of inter-annual variability of Atlantic hurricanes during the past decade. *Geophysical Research Letters*, *38*, L11804. https://doi.org/10.1029/2011GL047629

Cheng, L., Trenberth, K. E., Fasullo, J., Abraham, J., Boyer, T. P., von Schuckmann, K., & Zhu, J. (2018). Taking the pulse of the planet. *Eos*, *98*. https://doi.org/10.1029/2017EO081839

Cheng, L., Trenberth, K. E., Fasullo, J., Boyer, T., Abraham, J., & Zhu, J. (2017). Improved estimates of ocean heat content from 1960–2015. *Science Advances*, *3*. https://doi.org/10.1126/sciadv.1601545

Cheng, L., Zhu, J., & Sriver, R. L. (2015). Global representation of tropical cyclone-induced short-term ocean thermal changes using Argo data. *Ocean Science*, *11*, 719–741. https://doi.org/10.5194/os-11-719-2015

Dee, D. P., Uppala, S. M., Simmons, A. J., Berrisford, P., Poli, P., Kobayashi, S., et al. (2011). The ERA-Interim reanalysis: Configuration and performance of the data assimilation system. *Quarterly Journal of the Royal Meteorological Society*, *137*, 553–597.

Ellenrieder, T. (2017). Hurricane Harvey: Record-breaking floods inundate Houston. https://www.munichre.com/topics-online/en/2017/12/hurricane-harvey

Emanuel, K. (2003). Tropical cyclones, Annu. Rev. *Earth and Planetary Science*, *31*, 75–104.

Emanuel, K. (2005). Increasing destructiveness of tropical cyclones over the past 30 years. *Nature*, *436*, 686. https://doi.org/10.1038/nature03906

Emanuel, K. (2007). Environmental factors affecting tropical cyclone power dissipation. *Journal of Climate*, *20*, 5497–5509. https://doi.org/10.1175/2007JCLI1571.1

Emanuel, K. (2013). Downscaling CMIP5 climate models shows increased tropical cyclone activity over the 21st century. *Proceedings of the National Academy of Sciences*, *110*, 12,219–12,224. https://doi.org/10.1073/pnas.1301293110

Emanuel, K. (2015). Effect of upper-ocean evolution on projected trends in tropical cyclone activity. *Journal of Climate*, *28*, 8165–8170. https://doi.org/10.1175/JCLI-D-15-0401.1

Emanuel, K. (2017). Assessing the present and future probability of hurricane Harvey's rainfall. *Proceedings of the National Academy of Sciences*, *114*(48), 12,681–12,684. https://doi.org/10.1073/pnas.1716222114

Garner, A. J., Mann, M. E., Emanuel, K. A., Kopp, R. E., Lin, N., Alley, R. B., et al. (2017). Impact of climate change on New York City's coastal flood hazard: Increasing flood heights from the preindustrial to 2300 CE. *Proceedings of the National Academy of Sciences*, *114*(45), 11,861–11,866. https://doi.org/10.1073/pnas.1703568114

Huffman, G. J., Adler, R. F., Bolvin, D. T., & Gu, G. (2009). Improving the global precipitation record: GPCP version 2.1. *Geophysical Research Letters*, *36*, L17808. https://doi.org/10.1029/2009GL040000

Huffman, G. J., Bolvin, D. T., Braithwaite, D., Hsu, K., Joyce, R., & Xie, P. (2014). Integrated Multi-satellitE Retrievals for GPM (IMERG), version 4.4. *NASA's Precipitation Processing Center*, ftp://arthurhou.pps.eosdis.nasa.gov/gpmdata/

IPCC (2013). Climate change 2013: The physical science basis. In T. F. Stocker, et al. (Eds.), *Intergovernmental Panel on Climate Change* (1535 pp.). Cambridge, United Kingdom: Cambridge University Press.

Jaimes, B., Shay, L. K., & Uhlhorn, E. W. (2015). Enthalpy and momentum fluxes during Hurricane Earl relative to underlying ocean features. *Monthly Weather Review*, *143*, 111–131. https://doi.org/10.1175/MWR-D-13-00277.1

Kelly, P. M., & Adger, W. N. (2000). Theory and practice in assessing vulnerability to climate change and facilitating adaptation. *Climatic Change*, *47*, 325–352.
Kimmelman, M. (2017). Lessons from Hurricane Harvey: Houston's struggle is America's tale.12 Nov 2017; New York Times. https://nyti.ms/2hqXvd5
Knutson, T. R., McBride, J. L., Chan, J., Emanuel, K., Holland, G., Landsea, C., et al. (2010). Tropical cyclones and climate change. *Nature Geoscience*, *3*, 157–163.
Knutson, T. R., Sirutis, J. J., Zhao, M., Tuleya, R. E., Bender, M., Vecchi, G., et al. (2015). Global projections of intense tropical cyclone activity for the late twenty-first century from dynamical downscaling of CMIP5/RCP4.5 scenarios. *Journal of Climate*, *28*, 7203–7224. https://doi.org/10.1175/jcli-d-15-0129.1
Knutti, R., & Sedláček, J. (2012). Robustness and uncertainties in the new CMIP5 climate model projections. *Nature Climate Change*, *3*, 269–273. https://doi.org/10.1038/nclimate1716
Kunreuther, H. (2006). Disaster mitigation and insurance: Learning from Katrina. *The Annals of the American Academy of Political and Social Science*, *604*, 208–227.
Kunreuther, H., Heal, G., Allen, M., Edenhofer, O., Field, C. B., & Yohe, G. (2013). Risk management and climate change. *Nature Climate Change*, *3*, 447–450. https://doi.org/10.1038/nclimate1740
LaRow, T. E., Stefanova, L., Shin, D.-W., & Cocke, S. (2010). Seasonal Atlantic tropical cyclone hindcasting/forecasting using two sea surface temperature datasets. *Geophysical Research Letters*, *37*, L02804. https://doi.org/10.1029/2009GL041459
Lin, I., Chen, C., Pun, I., Liu, W., & Wu, C. (2009). Warm ocean anomaly, air sea fluxes, and the rapid intensification of tropical cyclone Nargis (2008). *Geophysical Research Letters*, *36*, L03817. https://doi.org/10.1029/2008GL035815
Lin, I., Chou, M., & Wu, C. (2011). The impact of a warm ocean eddy on typhoon Morakot (2009): A preliminary study from satellite observations and numerical modeling. *Terrestrial, Atmospheric and Oceanic Sciences*, *22*, 661–671.
Lin, I., Wu, C., Pun, I., & Ko, D. (2008). Upper-ocean thermal structure and the western North Pacific category 5 typhoons. Pt I: Ocean features and the category 5 typhoons' intensification. *Monthly Weather Review*, *136*, 3288–3306. https://doi.org/10.1175/2008MWR2277.1
Lin, N., & Shullman, E. (2017). Dealing with hurricane surge flooding in a changing environment: Part I. Risk assessment considering storm climatology change, sea level rise, and coastal development. *Stochastic Environmental Research and Risk Assessment*, *31*, 2379–2400. https://doi.org/10.1007/s00477-016-1377-5
Lloyd, I. D., & Vecchi, G. A. (2011). Observational evidence for oceanic controls on hurricane intensity. *Journal of Climate*, *24*, 1138–1153. https://doi.org/10.1175/2010JCLI3763.1
Loeb, N. G., Wielicki, B., Doelling, D. R., Smith, G. L., Keyes, D. F., Kato, S., et al. (2009). Toward optimal closure of the Earth's top-of-atmosphere radiation budget. *Journal of Climate*, *22*, 748–766.
Magnusson, L., Tsonevsky, I., & Prates, F. (2017). Predictions of tropical cyclones Harvey and Irma. *ECMWF Newsletter*, *153*, 4–5.
Mann, M., & Emanuel, K. (2006). Atlantic hurricane trends linked to climate change. *Eos*, *87*, 233–241. https://doi.org/10.1029/2006EO240001
Mei, W., & Pasquero, C. (2013). Spatial and temporal characterization of sea surface temperature response to tropical cyclones. *Journal of Climate*, *26*, 3745–3765. https://doi.org/10.1175/JCLI-D-12-00125.1
Mesinger, F., DiMego, G., Kalnay, E., Mitchell, K., Shafran, P. C., Ebisuzaki, W., et al. (2006). North American Regional Reanalysis. *Bulletin of the American Meteorological Society*, *87*, 343–360. https://doi.org/10.1175/BAMS-87-3-343
Morss, R. E., Wilhelmi, O. V., Meehl, G. A., & Dilling, L. (2011). Improving societal outcomes of extreme weather in a changing climate: An integrated perspective. *Annual Review of Environment and Resources*, *36*, 1–25.
NOAA (2017). Billion dollar weather and climate disasters. https://www.ncdc.noaa.gov/billions/events/US/1980%E2%80%932017
Peduzzi, P., Chatenoux, B., Dao, H., De Bono, A., Herold, C., Kossin, J., et al. (2012). Global trends in tropical cyclone risk. *Nature Climate Change*, *2*, 289. https://doi.org/10.1038/nclimate1410
Pinker, R. T., Bentamy, A., Katsaros, K. B., Ma, Y., & Li, C. (2014). Estimates of net heat fluxes over the Atlantic Ocean. *Journal of Geophysical Research: Oceans*, *119*, 1–18. https://doi.org/10.1002/2013JC009386
Prasad, T. G., & Hogan, P. J. (2007). Upper-ocean response to Hurricane Ivan in a 1/25 nested Gulf of Mexico HYCOM. *Journal of Geophysical Research*, *112*, C04013. https://doi.org/10.1029/2006JC003695
Price, J. F. (1981). Upper-ocean response to a hurricane. *Journal of Physical Oceanography*, *11*, 153–175.
Ramkissoon, H., & Kahwa, I. (2015). The Caricom countries. In: UNESCO Science Report: toward 2030. https://en.unesco.org/unesco_science_report.
Rayner, N. A., Parker, D. E., Horton, E. B., Folland, C. K., Alexander, L. V., Rowell, D. P., et al. (2003). Global analyses of sea surface temperature, sea ice, and night marine air temperature since the late nineteenth century. *Journal of Geophysical Research*, *108*(D14), 4407. https://doi.org/10.1029/2002JD002670
Risser, M. D., & Wehner, M. F. (2017). Attributable human-induced changes in the likelihood and magnitude of the observed extreme precipitation during Hurricane Harvey. *Geophysical Research Letters*, *44*, 12,457–12,464. https://doi.org/10.1002/2017GL075888
Rogers, R. F., Aberson, S., Bell, M. M., Cecil, D. J., Doyle, J. D., & Kimberlain, et al. (2017). Rewriting the tropical record books: The extraordinary intensification of Hurricane Patricia (2015). *Bulletin of the American Meteorological Society*, *98*, 2091–2112. https://doi.org/10.1175/BAMS-D-16-0039.1
Schneider, U., Becker, A., Finger, P., Meyer-Christoffer, A., Ziese, M., & Rudolf, B. (2014). GPCC's new land surface precipitation climatology based on quality-controlled in situ data and its role in quantifying the global water cycle. *Theoretical and Applied Climatology*, *115*, 15–40.
Shay, L. K., Black, P. G., Mariano, A. J., Hawkins, J. D., & Elsberry, R. L. (1992). Upper ocean response to Hurricane Gilbert. *Journal of Geophysical Research*, *97*, 20,227–20,248. https://doi.org/10.1029/92JC01586
Sitkowski, M., Kossin, J. P., Rozoff, C. M., & Knaff, J. A. (2012). Hurricane eyewall replacement cycle thermodynamics and the relict inner eyewall circulation. *Monthly Weather Review*, *140*, 4035–4045. https://doi.org/10.1175/MWR-D-11-00349.1
Sobel, A. H., Camargo, S. J., Hall, T. M., Lee, C.-Y., Tippett, M. K., & Wing, A. A. (2016). Human influence on tropical cyclone intensity. *Science*, *353*, 242–246. https://doi.org/10.1126/science.aaf6574
Sriver, R. L., & Huber, M. (2007). Observational evidence for an ocean heat pump induced by tropical cyclones. *Nature*, *447*, 577–580. https://doi.org/10.1038/nature05785
Stone, R. (2018). Cuba's 100-year plan for climate change. *Science*, *359*, 144–145.
Trenberth, K. E. (2005). Climate. Uncertainty in hurricanes and global warming. *Science*, *308*, 1753–1754. https://doi.org/10.1126/science.aac9225
Trenberth, K. E., Dai, A., Rasmussen, R. M., & Parsons, D. B. (2003). The changing character of precipitation. *Bulletin of the American Meteorological Society*, *84*, 1205–1217. https://doi.org/10.1175/bams-84-9-1205

Trenberth, K. E., Davis, C. A., & Fasullo, J. (2007). Water and energy budgets of hurricanes: Case studies of Ivan and Katrina. *Journal of Geophysical Research*, *112*, D23106. https://doi.org/10.1029/2006JD008303

Trenberth, K. E., & Fasullo, J. (2007). Water and energy budgets of hurricanes and implications for climate change. *Journal of Geophysical Research: Atmospheres*, *112*, D23107. https://doi.org/10.1029/2006JD008304

Trenberth, K. E., & Fasullo, J. (2008). Energy budgets of Atlantic hurricanes and changes from 1970. *Geochemistry, Geophysics, Geosystems*, *9*, Q09V08. https://doi.org/10.1029/2007GC001847

Trenberth, K. E., Fasullo, J., & Smith, L. (2005). Trends and variability in column-integrated atmospheric water vapor. *Climate Dynamics*, *24*, 741–758.

Trenberth, K. E., & Fasullo, J. T. (2013). Regional energy and water cycles: Transports from ocean to land. *Journal of Climate*, *26*, 7837–7851. https://doi.org/10.1175/JCLI-D-00008.1

Trenberth, K. E., & Fasullo, J. T. (2017). Atlantic meridional heat transports computed from balancing Earth's energy locally. *Geophysical Research Letters*, *44*, 1919–1927. https://doi.org/10.1002/2016GL072475

Trenberth, K. E., Fasullo, J. T., & Balmaseda, M. A. (2014). Earth's energy imbalance. *Journal of Climate*, *27*, 3129–3144. https://doi.org/10.1175/JCLI-D-13-00294

Trenberth, K. E., Fasullo, J. T., & Mackaro, J. (2011). Atmospheric moisture transports from ocean to land and global energy flows in reanalyses. *Journal of Climate*, *24*, 4907–4924. https://doi.org/10.1175/2011JCLI4171.1

Trenberth, K. E., Zhang, Y., Fasullo, J. T., & Taguchi, S. (2015). Climate variability and relationships between top-of-atmosphere radiation and temperatures on Earth. *Journal of Geophysical Research: Atmospheres*, *120*, 3642–3659. https://doi.org/10.1002/2014JD022887

USGCRP (2017). In D. J. Wuebbles, et al. (Eds.), *Climate science special report: Fourth National Climate Assessment* (Vol. I, p. 470). Washington, DC: U.S. Global Change Research Program. https://doi.org/10.7930/J0J964J6

van Oldenborgh, G. J., van der Wiel, K., Sebastian, A., Singh, R., Arrighi, J., Otto, F., et al. (2017). Attribution of extreme rainfall from Hurricane Harvey, August 2017. *Environmental Research Letters*, *12*, 124009.

Vecchi, G. A., & Soden, B. J. (2007). Effect of remote sea surface temperature change on tropical cyclone potential intensity. *Nature*, *450*, 1066. https://doi.org/10.1038/nature06423

Vecchi, G. A., Zhao, M., Wang, H., Villarini, G., Rosati, A., Kumar, A., et al. (2011). Statistical-dynamical predictions of seasonal North Atlantic hurricane activity. *Monthly Weather Review*, *139*, 1070–1082. https://doi.org/10.1175/2010MWR3499.1

Villarini, G., & Vecchi, G. A. (2012). North Atlantic Power Dissipation Index (PDI) and Accumulated Cyclone Energy (ACE): Statistical modeling and sensitivity to sea surface temperature changes. *Journal of Climate*, *25*, 625–637. https://doi.org/10.1175/jcli-d-11-00146.1

von Schuckmann, K., Palmer, M. D., Trenberth, K. E., Cazenave, A., Chambers, D., Champollion, N., et al. (2016). Earth's energy imbalance: An imperative for monitoring. *Nature Climate Change*, *6*, 138–144. https://doi.org/10.1038/NCLIM-15030445C

Walsh, K. J. E., Camargo, S. J., Vecchi, G. A., Daloz, A. S., Elsner, J., Emanuel, K., et al. (2015). Hurricanes & climate: The U.S. CLIVAR Working Group on Hurricanes. *Bulletin of the American Meteorological Society*, *96*, 997–1017. https://doi.org/10.1175/bams-d-13-00242.1

Wang, S.-Y. S., Zhao, L., Yoon, J.-H., Klotzbach, P., & Gillies, R. R. (2018). Attribution of climate effects on Hurricane Harvey's extreme rainfall in Texas. *Environmental Research Letters*, *13*. https://doi.org/10.1088/1748-9326/aabb85, in press

Yamada, Y., Satoh, M., Sugi, M., Kodama, C., Noda, A. T., Nakano, M., & Nasuno, T. (2017). Response of tropical cyclone activity and structure to global warming in a high-resolution global nonhydrostatic model. *Journal of Climate*, *30*, 9703–9724. https://doi.org/10.1175/jcli-d-17-0068.1

Yu, L., & Weller, R. A. (2007). Objectively analyzed air-sea heat fluxes (OAFlux) for the global ocean. *Bulletin of the American Meteorological Society*, *88*, 527–539.